Microelectronic Engineering 142 (2015) 36–39

Contents lists available at ScienceDirect

Microelectronic Engineering

journal homepage: www.elsevier.com/locate/mee

Short note

Measurement of out-of-plane thermal conductivity of substrates for flexible electronics and displays

Vivek Vishwakarma, Chirag Waghela, Ankur Jain *

Mechanical and Aerospace Engineering Department, University of Texas at Arlington, 500 W First St., Arlington, TX 76019, USA

ARTICLE INFO

Article history:
Received 7 April 2015
Received in revised form 12 June 2015
Accepted 26 June 2015
Available online 18 July 2015

Keywords:
Flexible electronics
Flexible displays
Substrate materials
Thermal management
Out-of-plane thermal conductivity

ABSTRACT

Thin, compliant substrates are increasingly being used for flexible electronics, displays, wearable devices, etc. The dissipation of heat generated in such devices is likely to be an important technological challenge that has not been investigated sufficiently. This paper reports measurement of the out-of-plane thermal conductivity of materials for thin substrates, which is a key material property that governs thermal performance. One-dimensional, steady state thermal conduction is set up in the substrate of interest. Measurements of temperature gradient induced by an imposed heat flux result in the determination of out-of-plane thermal conductivity. Thermal contact resistance between the substrate and experimental setup is also obtained. Measurements are carried out on polyethylene naphthalate (PEN) and polyethylene teraphthalate (PET) substrates of varying thicknesses. Based on the measured thermal conductivity, simulations are carried out to compare the thermal performance of a thin substrate with a traditional substrate. Though flexible electronic devices dissipate very less power, the low thermal conductivity measured here, and the low substrate thickness indicate the critical need for thermal management of such devices. Results reported here indicate an upper limit on power dissipation in a flexible device compared to a traditional device for maintaining similar thermal performance. Measurements reported in this paper may help in the fundamental understanding of thermal transport and thermal management strategies in flexible electronics and displays.

1. Introduction

While traditional microelectronic devices are manufactured on thick, hard substrates, there has been a lot of recent interest in thin substrates, with applications including flexible displays [1,2], wearable electronics [3,4], electronic textiles [4], sensors skins [5,6], and thin-film transistors (TFTs) [7–11]. Substrate thickness for such devices can be as low as 25 μm [1]. As these technologies evolve, there will be a need to evaluate the thermal management of these devices. Even though such devices typically generate very less power compared to traditional electronic devices, there are likely to be several thermal management concerns. The dramatically reduced substrate thickness hinders heat spreading. Non-traditional substrates such as plastics introduce additional thermal concerns, such as low thermal conductivity [1,2], excessive thermal expansion, and low glass transition temperature [12]. The unavailability of traditional thermal management tools such as heat sinks and heat pipes may further exacerbate the challenge of thermal management in such applications. As the complexity and power consumption of flexible devices is expected to increase in the future [13,14], it is critical to understand the nature of thermal transport in these substrate materials and establish power limits to ensure device reliability.

Thermal conductivity is a key material property that determines the thermal performance of devices and substrates [15]. In general, thermal conductivity may be anisotropic, depending, for example, on grain orientation for crystalline materials [16]. In the case of substrates for electronic devices, the out of plane thermal conductivity may be more critical, since it directly affects thermal conduction from the device to the substrate backside, from where it may be dissipated into the ambient. A number of experimental techniques exist for thermal conductivity measurements on electronic materials [15–18]. These methods are usually based on steady-state, transient or periodic heating of the test material, and measurement of subsequent temperature rise at one or multiple locations [15–18]. Both electrical and optical methods for heating and temperature detection have been investigated [15]. Within electrical methods, both DC and AC-based methods have been used [19–23]. Separate methods have addressed either relatively thick substrates (hundreds of μm or thicker) [22], or thin films (a few μm or thinner) deposited on a thick substrate [21,23]. Sinusoidal heating of a thick substrate with a thermal penetration depth smaller than substrate thickness has been used widely [22]. Thermal conductivity of thin films has been measured based on the difference in thermal response of a thick substrate with and without the thin film [21]. Thermal conductivity of free-standing thin films has also been measured [18]. However,

* Corresponding author.
E-mail address: jaina@uta.edu (A. Jain).

http://dx.doi.org/10.1016/j.mee.2015.06.008
0167-9317/

there is a lack of experimental measurements on thin substrates in the thickness range of a few tens of μm, for which methods for neither thick substrates nor thin films are appropriate. For example, the use of 3-ω method [22] for this thickness range would require unrealistically large heating frequencies. While bulk-form thermal conductivity has been measured in the past for materials commonly used for thin substrates such as polyethylene naphthalate (PEN) and polyethylene teraphthalate (PET), an in situ measurement on substrates of the thickness of interest to flexible devices – a few tens of μm – is desirable, since thermal conductivity is known to depend strongly on processing conditions [15].

In this paper, one-dimensional steady-state thermal conduction is set up in a substrate of interest for measurement of out-of-plane thermal conductivity of the substrate. Temperature and heat flux measurements are used to determine total thermal resistance of the substrate. Measurements on multiple substrates of the same material but different thicknesses result in determination of thermal conductivity of the substrate.

The next section describes the experimental setup. Data analysis and results are presented next, followed by a discussion on the implications of the measured thermal conductivity on thermal management of flexible electronic devices.

2. Experiments

Fig. 1 shows an image and a schematic of the experimental setup. The setup utilizes two identical copper blocks. The substrate of interest is sandwiched between the two blocks. The two faces of copper blocks that come in contact with the substrate are polished in a two-step process, using a 120 grit sandpaper belt on a LECO BG-30 polisher, followed by a 1200 grit sandpaper drenched with 0.05 μm alumina microparticles on LECO VP-150 polisher. A thin Kapton heater of the same size as the block cross-section is attached to the face opposite to the polished surface of one of the blocks. A through-hole is drilled close to the face opposite to the polished surface of the other block. This through-hole is connected to flexible tubing carrying cooling water from a chiller. Seven holes of 1.0 mm diameter extending to the center of the block are drilled along the length of each block. The holes are spaced closer to each other near the polished surfaces. T-type thermocouples are inserted all the way into the holes to measure the block temperature as a function of distance in each block. Holes are drilled along expected isotherms in order to minimize heat loss down the thermocouple wires. Based on the thermocouple wire dimensions and material, and the maximum temperature reached during experiments, the worst-case heat loss due to thermal conduction down the thermocouple wires is estimated to be only 0.2% of the applied heat. Omega CC High Temperature cement is used to fix thermocouples in place and provide good thermal contact with the copper block. All faces of the copper blocks except the polished faces are then insulated with fiberglass insulation tape. The Kapton heater attached to the top block is electrically heated using a power source. A Keithley 2100 digital multimeter is used to monitor voltage across the heater. Electrical resistance of the heater is found to remain nearly constant within the temperature range of this experiment. Thus, the heater provides a constant heat flux through the experiment.

Temperature measurements are recorded with 1 Hz frequency through a National Instruments 9213 DAQ and LabView software. Fig. 2 plots the measured temperature at steady-state as a function of distance away from the heater end for PEN substrates of different thicknesses. In each case, the temperature profiles in the top and bottom heater are both linear, with nearly the same slope. This indicates linear, one-dimensional heat flow in the experiment. The offset between the two lines when extrapolated to the interface location determines the temperature difference across the two heater blocks. Figure S.1 in Supplementary Information plots the temperature difference as a function of time after initiation of heating for five different substrate thicknesses. This plot shows that temperature difference across the blocks increases with time, and eventually reaches steady state, at which time all heat generated in the heater conducts through the copper blocks, and no heat is stored within. Steady state is reached in these experiments typically within 1300 s.

3. Results and discussion

At steady state, the total thermal resistance across the copper blocks, R_{total} is obtained from

$$R_{total} = \frac{\Delta T}{Q} \tag{1}$$

where ΔT is the steady state temperature difference across the interface and Q is the heat flux. Q can be obtained from Fourier's law using the measured temperature slope dT/dx in the two copper blocks.

Note that R_{total} includes contributions from material thermal resistance in the substrate, R_{subs} and thermal contact resistance at the interface between copper and substrate, $R_{Cu\text{-}subs}$. The relative proportion of these

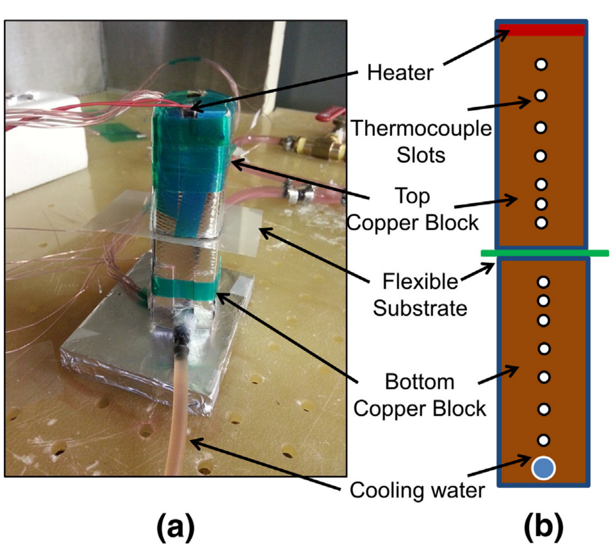

Fig. 1. (a) Image, and (b) schematic of the experimental measurement setup for out of plane thermal conductivity measurement of a flexible substrate.

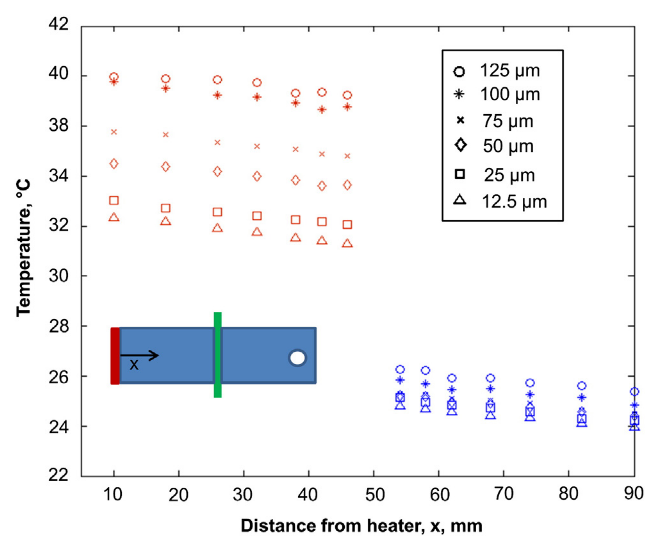

Fig. 2. Measured temperature as a function of distance away from heater for 25 μm PEN substrate.

contributions is not known since $R_{Cu\text{-}subs}$ depends on surface roughness and the micro-mechanics of how the surfaces come in contact with each other [24,25], whereas R_{subs} depends on the substrate thermal conductivity, which is the quantity of interest. In general,

$$R_{total} = 2R_{Cu-subs} + \frac{L_{subs}}{k_{subs}} \tag{2}$$

where L_{subs} and k_{subs} are the thickness and thermal conductivity of the substrate respectively. Note the factor of 2 in Eq. (2) due to the presence of two interfaces between copper and the substrate.

Since $R_{Cu\text{-}subs}$ is not known in advance, measurement of ΔT and Q is required for substrates of different thicknesses. Fig. 3 plots R_{total} as a function of L_{subs} for PEN and PET substrates, which are widely used for flexible electronics [1,2]. L_{subs} is measured using Vernier calipers. Fig. 3 shows a linear variation of R_{total} with L_{subs} for both substrates, as expected from Eq. (2). Thermal conductivity of the substrate material is determined from the inverse of the slope of the linear curve in Fig. 3. On the other hand, $R_{Cu\text{-}subs}$ is determined as half of the y-intercept of the curve. Table 1 summarizes the measured values of k_{subs} and $R_{Cu\text{-}subs}$ for PEN and PET films. The somewhat low values of k_{subs} obtained from these measurements, while expected for plastic-based substrates, have significant impact on thermal modeling and management of flexible substrates, as discussed later in this paper. A 15% measurement uncertainty is estimated for the measurements summarized in Table 1.

For further validation of the measurements, experiments are repeated while applying external pressure on the interface. Metal weights are placed on top of the experimental setup. Variation of R_{total} with L_{subs} with 7.4 kPa external pressure is also shown in Fig. 3 for both PEN and PET films. Compared to the case with no external pressure, these curves have approximately the same slope, but much lower y-intercept. This indicates, as expected, that the application of external pressure leads to reduction in $R_{Cu\text{-}subs}$, because of a more intimate contact between the two surfaces. $R_{Cu\text{-}subs}$ reduces to 139 and 212 μK·m^2/W for PEN and PET respectively. On the other hand, k_{subs}, which is related to the slope of the curve remains relatively unaffected by pressure. This is also expected, since k_{subs} is an inherent material property of the substrate, which should be largely independent of pressure.

As an alternate to the approach of measuring R_{total} on substrates of different thicknesses, experiments are also carried out on stacks of multiple substrate samples of the same thickness. Comparison of R_{total} as a function of total thickness for both approaches for PEN substrate

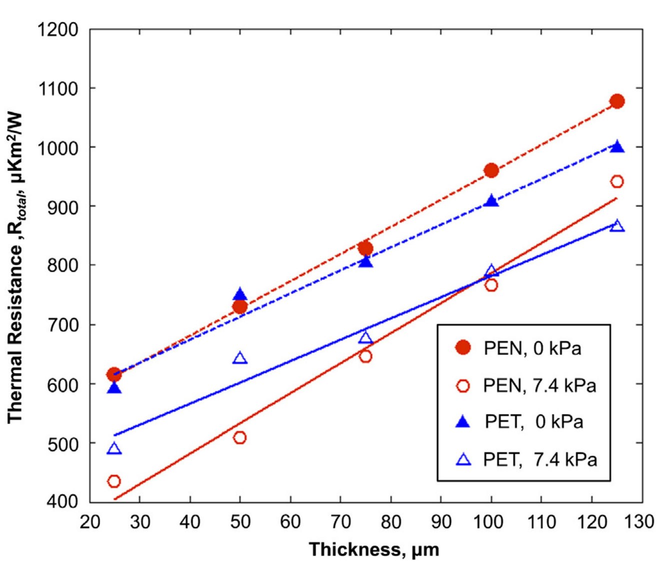

Fig. 3. Measured total thermal resistance for PEN and PET substrates as a function of substrate thickness, for 0 and 7.4 kPa external pressure.

Table 1
Measured thermal conductivity and thermal contact resistance (TCR) of PEN and PET films to copper. A 15% uncertainty is estimated for these data.

	k (W/m·K)	$R_{Cu\text{-}Subs}$ (μK·m^2/W)
PEN	0.22	248
PET	0.26	260

is included in Fig. S.2 in Supplementary information. It is found that R_{total} is higher when multiple substrates are stacked together to obtain a certain thickness compared to using a single substrate of the same thickness. This is due to the additional thermal contact resistance incurred when substrates are stacked on each other. The larger the number of substrates in the stack, the larger is the expected additional thermal contact resistance compared to a single thickness substrate. This is seen in Fig. S.2 where the gap between the two sets of data widens as total thickness increases. Experiments are also carried out on 100 μm total thickness obtained from either a single 100 μm thick substrate, or two 50 μm thick substrates, or four 25 μm thick substrates. As expected, R_{total} is found to be the highest for the third case (1200 μK·m^2/W), lower for the second case (1080 μK·m^2/W) and lowest for the first case (961 μK·m^2/W).

Note that the measurement of k_{subs} outlined above depends upon the availability of substrates of different thicknesses, since stacking multiple samples to increase overall thickness results in introduction of additional, unknown thermal resistance. It is also assumed that different samples offer the same thermal contact resistance to copper, which may be reasonable if the samples are manufactured with similar surface finish.

Flexible electronic devices are likely to be used primarily for display-related functions, which dissipate much lesser power compared to traditional, computation-intensive electronics [13,14]. However, the poor thermal conductivity measured here, compared to substrates for traditional electronics such as silicon, and the lack of active cooling are expected to present challenges in thermal management of flexible electronics. Further, the ultra-low thickness may also contribute to the thermal challenge by preventing heat spreading from local regions of high heat dissipation. Finite-element thermal simulations are carried out to compare thermal performance of flexible electronic devices fabricated on PEN and PET substrates with traditional electronics on a thick silicon substrate. These simulations quantify the impact of factors listed above on the thermal performance of flexible electronics. Mechanical deformation due to thermal expansion is neglected, since the effect of the small change in substrate shape and dimensions is likely to have only a negligible effect on the temperature field. Fig. 4 compares a 25 μm electronic device (device A) with a 750 μm silicon-based traditional electronic device (device B). Thermal conductivity measured for PEN in this work is used for device A. Both substrates are 10 mm by 10 mm in size. A heat generation hotspot of size 1 mm by 1 mm dissipating 1.0 W/mm^2 is assumed to be located at the center of device B. A similarly sized hotspot at the same location, but with much lower power of 0.001 W/mm^2 is assumed for device A. While a traditional heat sink is modeled on the backside of device B, device A is assumed to be cooled entirely through natural convection. The impact of thermal contact resistance between the device and substrate, while important in general, can be neglected here, since typical device fabrication processes such as transfer printing are designed for good adherence [26], and hence good thermal contact between the device and the substrate. The effect of strain on heat generation or physical size of device A is also neglected, since realistic strains in flexible devices are not expected to significantly affect power generation or substrate size. Results indicate that despite the much lower power in device A, the temperature rise is comparable to the traditional device B. Simulation results indicate that for conditions outlined above, the flexible device may dissipate no more than 0.1% of the power dissipated in the traditional device to maintain the same temperature rise as the traditional device. These

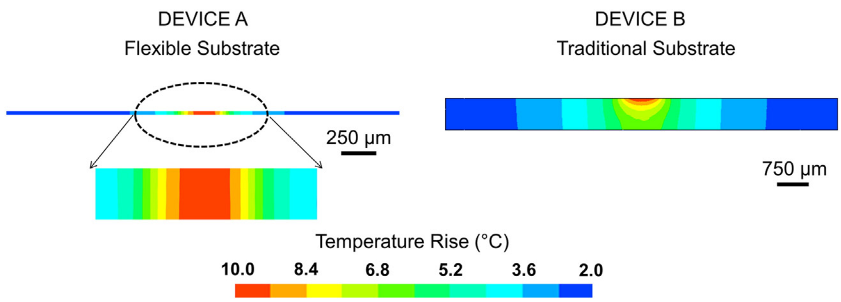

Fig. 4. Comparison of temperature distribution in flexible substrate and traditional substrate, based on measured thermal conductivity.

simulations and measurements may also be important to account for glass transition that these substrates undergo at fairly low temperature [12]. This provides a thermally-driven limit on computation capability of flexible electronic devices. It is imperative to recognize the thermal challenges due to low thermal conductivity reported here, and accordingly develop effective thermal management strategies.

4. Conclusions

In conclusion, this paper presents measurements of out of plane thermal conductivity of substrates of relevance to flexible electronic devices. Measurements of the total thermal resistance on substrates of different thicknesses result in determination of the thermal conductivity as well as thermal contact resistance. The measured thermal conductivity is quite poor, indicating the need for thermal management of future flexible electronics that may dissipate significant heat. The simulations presented in this paper highlight the trade-offs between flexible and traditional substrates due to differences in the thickness, power dissipation and availability of traditional thermal management strategies. Results indicate that a flexible electronics device may not dissipate more than around 0.1% of the power dissipated in a traditional device for comparable thermal performance. The measurement and simulation results presented here may help understand thermal management challenges, and may help ensure high performance and reliability through effective dissipation of heat.

Appendix A. Supplementary data

Supplementary data to this article can be found online at http://dx.doi.org/10.1016/j.mee.2015.06.008.

References

[1] G.H. Gelinck, H.E. Huitema, E. van Veenendaal, E. Cantatore, L. Schrijnemakers, J.B.P.H. van der Putten, T.C.T. Geuns, M. Beenhakkers, J.B. Giesbers, B.-H. Huisman, E.J. Meijer, E.M. Benito, F.J. Touwslager, A.W. Marsman, B.J.E. van Rens, D.M. de Leeuw, Flexible active-matrix displays and shift registers based on solution-processed organic transistors, Nat. Mater. 3 (2004) 106.
[2] L. Zhou, A. Wanga, S.C. Wu, J. Sun, S. Park, T.N. Jackson, All-organic active matrix flexible display, Appl. Phys. Lett. 88 (2006) 083502.
[3] S. Jung, C. Lauterbach, M. Strasser, W. Weber, Enabling technologies for disappearing electronics in smart textiles, Proc. IEEE Int. Solid State Circ. Conf. 1 (2003) 386.
[4] S. Park, S. Jayaram, Smart textiles: smart wearable electronics, MRS Bull. 28 (2003) 585.
[5] J. Engel, J. Chen, C. Liu, Development of polyimide flexible tactile sensor skin, J. Micromech. Microeng. 13 (2003) 359.
[6] Y. Xu, Y. Tai, A. Huang, C. Ho, IC-integrated flexible shear-stress sensor skin, J. Microelectromech. Syst. 12 (2003) 740.
[7] Y. Kim, D. Moon, J. Han, Organic TFT array on a paper substrate, IEEE Electron Device Lett. 25 (2004) 702.
[8] K. Nomura, H. Ohta, A. Takagi, T. Kamiya, M. Hirano, H. Hosono, Room-temperature fabrication of transparent flexible thin-film transistors using amorphous oxide semiconductors, Nature 432 (2004) 488.
[9] H. Sirringhaus, Device physics of solution-processed organic field-effect transistors, Adv. Mater. 17 (2005) 2411.
[10] E. Artukovic, M. Kaempgen, D.S. Hecht, S. Roth, G. Grüner, Transparent and flexible carbon nanotube transistors, Nano Lett. 5 (2005) 757.
[11] H. Sirringhaus, T. Kawase, R.H. Friend, T. Shimoda, M. Inbasekaran, W. Wu, E.P. Woo, High-resolution inkjet printing of all-polymer transistor circuits, Science 290 (2000) 2123.
[12] C.E. Wilkes, J.W. Summers, C.A. Daniels, T. Berard, PVC Handbook, 1st ed. Hanser Publishing Co., 2005
[13] M. Zirkl, A. Haase, A. Fion, H. Schön, C. Sommer, G. Jakopic, G. Leising, B. Stadlober, I. Graz, N. Gaar, R. Schwödiauer, S. Bauer-Gogonea, S. Bauer, Low-voltage organic thin-film transistors with high-k nanocomposite gate dielectrics for flexible electronics and optothermal sensors, Adv. Mater. 19 (2007) 2241.
[14] T. Huang, K. Cheng, Design for low power and reliable flexible electronics: self-tunable cell-library design, J. Disp. Technol. 5 (2009) 206.
[15] D.G. Cahill, K. Goodson, A. Majumdar, Thermometry and thermal transport in micro/nanoscale solid-state devices and structures, J. Heat Transf. 124 (2002) 223.
[16] K. Kurabayashi, M. Asheghi, M. Touzelbaev, K.E. Goodson, Measurement of the thermal conductivity anisotropy in polyimide films, J. Microelectromech. Syst. 8 (1999) 180.
[17] L. Shi, D. Li, C. Yu, W. Jang, D. Kim, Z. Yao, P. Kim, A. Majumdar, Measuring thermal and thermoelectric properties of one-dimensional nanostructures using a microfabricated device, J. Heat Transf. 125 (2003) 881.
[18] A. Jain, K.E. Goodson, Measurement of the thermal conductivity and heat capacity of freestanding shape memory thin films using the 3ω method, J. Heat Transf. 130 (2008) 102402.
[19] S.E. Gustafsson, Transient plane source techniques for thermal conductivity and thermal diffusivity measurements of solid materials, Rev. Sci. Instrum. 62 (1991) 797.
[20] X. Hu, L. Jiang, K.E. Goodson, Thermal conductance enhancement of particle-filled thermal interface materials using carbon nanotube inclusions, Proc. 9th Intersoc. Conf. Therm. Thermomechanical Phenom, Electron. Syst., 63, 2004.
[21] D.G. Cahill, M. Katiyar, J.R. Abelson, Thermal conductivity of a-Si:H thin films, Phys. Rev. 50 (1994) 6077.
[22] D.G. Cahill, Thermal conductivity measurement from 30 to 750 K: the 3ω method, Rev. Sci. Instrum. 61 (1990) 802.
[23] D.G. Cahill, Thermal conductivity of thin films: measurements and understanding, J. Vac. Sci. Technol. A 7 (1989) 1259.
[24] M.G. Cooper, B.B. Mikic, M.M. Yovanovich, Thermal contact conductance, Int. J. Heat Mass Transf. 12 (1969) 279.
[25] M.M. Yovanovich, Four decades of research on thermal contact, gap, and joint resistance in microelectronics, IEEE Trans. Compon. Packag. Technol. 28 (2005) 182.
[26] M. Berggren, D. Nilsson, N.D. Robinson, Organic materials for printed electronics, Nat. Mater. 6 (2007) 3.